

Experimental study and numerical investigation of behavior of RC beams strengthened with steel reinforced grout

Francesco Bencardino* and Antonio Condello

*Department of Civil Engineering, University of Calabria,
Via P. Bucci, Cubo 39B, 87036 Rende, Cosenza, Italy*

(Received March 20, 2014, Revised July 7, 2014, Accepted October 10, 2014)

Abstract. The purpose of this study is to evaluate the behavior and the strength of SRG (Steel Reinforced Grout) externally strengthened Reinforced Concrete (RC) beams by using a nonlinear numerical analysis. The numerical simulation was carried out by using a three-dimensional (3D) finite element model. An interface element with a suitable damage model was used to model the connection between concrete surface and SRG reinforcing layer. The reliability of the finite element 3D-model was checked using experimental data obtained on a set of three RC beams.

The parameters taken into consideration were the external configuration, with or without U-end anchorages, the concrete strength, the amount of internal tensile steel reinforcement.

Conclusions were made concerning the strength and the ductility of the strengthened beams by varying the parameters and on the effectiveness of the SRG reinforcing system applied with two types of external strengthening configuration.

Keywords: finite element method; non-linear analysis; reinforced concrete; steel reinforced grout; strengthening

1. Introduction

The numerous experimental and numerical studies available in the literature have clearly evidenced the capability of fiber reinforced polymer materials (FRP) in improving the structural performances of reinforced concrete (RC) beams (Ebead and Saeed 2014, Demakos *et al.* 2013, Jumaat and Ashrafual Alam 2010, Lu *et al.* 2005a, Bencardino *et al.* 2005, Bencardino *et al.* 2002). Other studies specifically investigated the interaction mechanisms between FRP strengthening systems and the support (Zhang and Teng 2010, Ferracuti *et al.* 2006, Lu *et al.* 2005b). Despite the results emerged from these studies the composite materials are still object of investigation, they have substantially contributed to the development of theoretical models at the basis of design formulas included in standard documents and design guidelines such as CNR-DT 200 R1 (2013), ACI 440.2R-08 (2008), ISIS Design Manual No. 4 (2008), Fib 35 (2006), Fib 14 (2001).

Although FRP systems are extensively used, their high cost and flammability are limitations that would be desirable to overcome. A new family of composite materials made of high-strength

*Corresponding author, Assistant professor, E-mail: francesco.bencardino@unical.it

carbon steel fiber reinforcing mesh impregnated with polymeric resin or cementitious grout has been recently introduced in the building market: steel reinforced polymer (SRP) and steel reinforced grout (SRG) systems (Huang *et al.* 2004, Casadei *et al.* 2005a). These systems are capable of ensuring the same advantages of the FRP systems, as the easiness of application, the low invasiveness and a reduced intervention time, but with a lower cost and a better fire resistance compared to that of the FRP materials. Moreover, the SRG system showed a high compatibility with traditional materials. Although some studies have been developed to evaluate properties and potential application of these new materials (Lopez *et al.* 2007, Pecce *et al.* 2006, Prota *et al.* 2006, Barton *et al.* 2005, Casadei *et al.* 2005b, Wobbe *et al.* 2004), currently, proper standard documents or guidelines for the design of externally bonded SRG/SRP systems for strengthening existing structures are not available.

In order to give a contribution to this topic an experimental and numerical analysis with reference to external strengthened RC beams with a SRG system, with and without U-end anchorages, was carried out. Through an appropriate numerical investigation, based on a suitable three-dimensional model, compared with the results of an experimental investigation, a parametric study was also developed. This has allowed to evaluate numerically the behavior of strengthened RC beams subjected to increasing static load up to failure, highlighting the effective reliability of the external reinforcement to varying of some main mechanical parameters, without having to measure experimentally.

2. Experimental program

2.1 Tested beams and materials

Three simply supported RC beams with different external arrangements have been tested and analyzed. Specifically, an ordinary RC beam without external reinforcement, labeled Beam A0, a beam externally strengthened with a layer of SRG applied to the bottom tensile face with supplementary “U” anchors placed near the supports in the cut-off zone of the SRG system (Beam A1.A) and, lastly, a beam strengthened only to flexure with a layer of SRG applied to the bottom tensile face (Beam A1.B). The use of U-end anchorages in the cut-off zone of external strengthening system are useful to optimize the structural performance of the strengthened beams in terms of strength, ductility, material strains and failure mode as showed in Spadea *et al.* 2000 and Bencardino *et al.* 2007.

All the three beams had a total length of 3000 mm, a cross section of 150 mm x 250 mm and were internally reinforced, both longitudinally and transversely, with the same amount of steel reinforcement. Specifically, two ribbed bars of 10 mm diameter were used for tension steel and two ribbed bars of 8 mm diameter were used for compression steel. The vertical stirrups were ribbed bars of 8 mm diameter spaced at 150 mm with a clear concrete cover of 20 mm. The Figs. 1(a)-(b) show the strengthened beams A1.A and A1.B with the external configuration details.

All the beams were tested under four point bending with a clear span of 2700 mm and a shear span-to-depth ratio of 4.15. The Figs. 2(a)-(b) show the control beam A0 with the geometrical dimensions and the internal steel reinforcement of the three beams, respectively.

The material used was a steel with a mean yield strength of 604.20 MPa and 496.00 MPa for the bars of diameter 10 mm and 8 mm, respectively. The mean values were evaluated on three bar samples for each diameter. The average concrete compressive cylinder strength evaluated

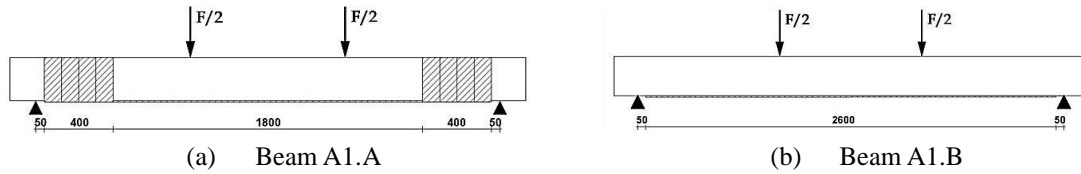


Fig. 1 RC beams strengthened with a SRG system

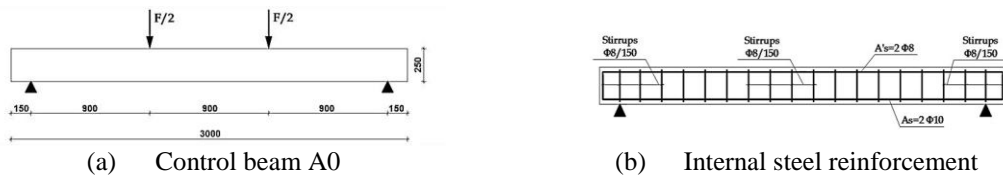


Fig. 2 Control Beam and internal steel reinforcement

at 28 days on six standard samples (150 mm × 300 mm) was 34.0 MPa and the average tensile split strength was 3.5 MPa. The maximum coarse aggregate size used in the concrete mix was 20 mm.

2.2 Properties of SRG system and bonding procedure

Before the bonding of the external reinforcement system, the bottom surface of the beams were cleaned to remove dust, loose parts and other elements. To promote adhesion a bi-component epoxy resin with the primer function was applied. For SRG reinforcement system the Kimisteel LM mortar mixed 30% by weight with a synthetic resin (Kimitech B2) was used. The unidirectional high-strength carbon steel fiber reinforcing mesh (Kimisteel 1500) with a width of 150 mm and a total length of 2600 mm was bonded using a grout matrix that was applied to the substrate using a smooth metal trowel in a layer about 2-3 mm thick. The fabric strip was lied on it and pressed lightly using a metal spreader to ensure the complete sinking of the fabric into the

Table 1 Properties of SRG system

Kimisteel 1500	
Total weight of fabric	1528 g/m ²
Fiber direction warp – steel	99 %
Fiber direction warp (weft)	1 %
Diameter steel chord (braid diameter)	1.07 mm
Rated tape thickness (steel only)	0.19 mm
Fiber tensile strength (breaking stress UHTSS)	2950 MPa
Unitary resistance	570 N/mm
Elastic tensile stress modulus (UHTSS)	260 GPa
Kimisteel LM + Kimitech B2	
Specific weight of mortar	1750 kg/m ³
Compression strength at 28 days	> 45 MPa
Flexural strength at 28 days	> 8 MPa
Concrete adhesion	> 2 MPa

matrix. A second layer of inorganic matrix about 2-3 mm thick was applied to cover the strip completely. The main properties of the SRG composite system, as supplied by the manufacturer and trading company (Kimia S.p.A. 2009), are shown in Table 1.

2.3 Instrumentation

All the beams were internally and externally instrumented, consequently, the applied load, the vertical displacements, and the material strains were monitored throughout the tests. Using the Linear Variable Displacement Transducers (LVDTs) the vertical displacements of the beams were measured at mid-span, at the applied load points and at half of the shear spans. Material strains were recorded using strain gages attached to the internal reinforcing bars, onto the top concrete surface in compression, and by eleven strain gages distributed along the length of the strip of the SRG system. The load was applied monotonically using a load cell. All data from load cell, strain gages, and LVDTs were recorded through a data acquisition system.

3. Finite element modeling

3.1 Three-dimensional FE model

The tested beams have been modeled using a finite element (FE) specialistic software (LUSAS “Finite Element Analysis Ltd”, version 14.5, 2010). It is worthwhile noting that a three-dimensional (3D) modeling has been carried out, without exploiting the symmetry conditions of constraint and of the load, that would allow significant simplifications. Mainly, this choice is due to the possibility to change, in analysis and design applications, the constraint conditions and the load that would remove the symmetry and, therefore, require a new modeling of the structural element. A 3D view of the model with the mesh is given in Figs. 3(a)-(b). Specifically, Fig. 3a shows the strengthened beam with one layer of SRG and additional U-end anchorages and Fig. 3b shows the RC beam strengthened by using only one SRG layer.

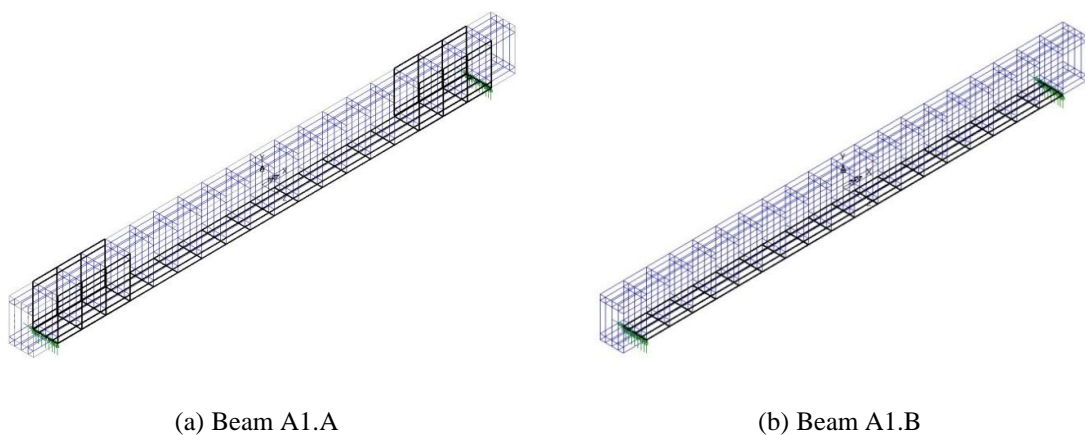


Fig. 3 FE mesh

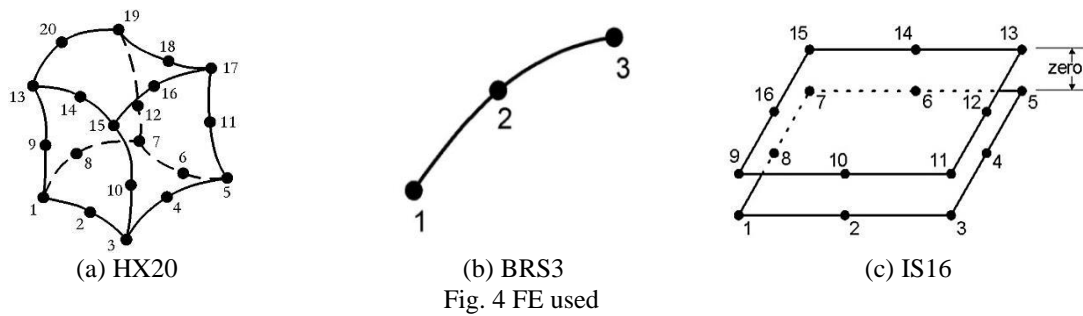


Fig. 4 FE used

3.2 Type of elements

In order to model the concrete and the external reinforcement the finite element HX20 has been used. It is an isoparametric continuum three dimensional element with 20 nodes, with three degrees of freedom for each node, represented by the displacements u , v , w in the three orthogonal directions with the Gauss quadratic interpolation $3 \times 3 \times 3$.

For the reinforcing bar the BRS3 element has been used, corresponding to a linear 3D element with three nodes. This element transfers only axial stress and has no flexural stiffness. The variables are the nodal displacements u , v and w , mutually orthogonal. The cross section area coincide with the reinforcement bars area: transversal or longitudinal. The superposition of the nodal degrees of freedom at the steel/concrete interface assumes that a perfect bond exists between the two components.

In order to model the concrete/external reinforcement interface, the element IS16 has been used. It is a 16 nodes element, with no thickness, that follows the 3×3 Newton-Cotes integration pattern. This element, inserted at the surfaces of potential delamination (bottom face of the strengthened beams and in the U-end anchorage zones), is particularly suitable for modeling the interlaminar failure, with the beginning and the propagation of cracks (Bencardino and Spadea 2014).

The Figs. 4(a)-(c) show the FE used in the model (HX20, BRS3, IS16).

3.3 Solution technique

The nonlinear load-displacement relationship requires an incremental-iterative procedure in which the load is gradually increased and equilibrium is iteratively searched for each increment. In this study the Modified Newton-Raphson method was adopted. Through this method, for each iteration the tangent stiffness matrix is replaced with a previous stiffness matrix, corresponding to that of the first iteration. The convergence rate of Modified Newton-Raphson is not quadratic and the procedure often diverges. With the purpose of improving the convergence speed, the method has been coupled with the “line search” technique that operates on single iteration, in the case in which localized nonlinearity are present.

When using an incremental-iterative procedure a measure of the convergence of the solution is required to define when the equilibrium has been achieved. The assignment of the tolerance values is closely linked to the experience, but in general, with predominantly materially nonlinear problems a slack tolerance is more effective, because high local residuals may have to be tolerated without compromising the accuracy of the solution. In this analysis reference was made to the

following convergence criteria: Euclidian residual norm ($rdnorm=0.1$), Euclidian displacement norm ($dpnorm=1.0$), Euclidian incremental displacement norm ($dtnrm=1.0$), Work norm ($wdnrm=10^8$), Root mean square of residuals ($RMS=10^8$), Maximum absolute residual ($MAR=10^8$). The generic load increment converges if the tolerance limit imposed is satisfied for each one of the parameters listed above.

An uniform load incrementation, fixed to 1000 N, was used. Where an increment failed to converge within a step load with the specified maximum number of iterations (set to 25), it was reduced and re-applied (reduction factor set to 0.5). This was repeated according to values specified in the step reduction section, until the maximum number of reductions has been tried. With an incremental procedure, the solution progresses one nonlinear control stage at a time. The finish of each nonlinear control stage is controlled by its termination parameters. The termination was specified by limiting the maximum value of a named freedom. It was chosen the maximum displacement of a point on the middle section (control point), set between 70 mm and 85 mm. Reached this value the analysis is stopped. Furthermore, if for each load increment are not met strain limits of the materials constituting the structural element, the arrest of the analysis could occur even before reaching the maximum displacement of the control point.

3.4 Materials

3.4.1 Concrete

The model used for the concrete is the “multi-crack model” that takes into account the nonlinear behavior in tension and compression, cracking and crushing. The concrete material model enables the nonlinear stress/strain behavior of concrete structures to be modeled to failure. It simulates multiple non-orthogonal cracking with exponential softening that can be linked to either a fracture energy parameter (G_F) or to a fixed limiting strain parameter (ϵ_0) (Bazant and Oh 1983). It is able to simulate crack closure in both shear, due to aggregate interlock, and compression. The model simulates nonlinear behavior in compression and diffuse cracking degradation associated with crushing by reduction of the first fracture stress. Quadratic convergence ensures that the number of iterations are minimized. It requires a relatively small number of material parameters, where each can be directly related to a physical characteristic.

The input parameters for the elastic phase are the Young modulus ($E_c=31760$ MPa), calculated according to relationship provided by Eurocode 2 (2004), and the Poisson ratio ($\nu_c=0.2$). For the plastic phase is considered the capacity of the cracked concrete to transmit tensile stresses (strain softening) as well as the ability to transfer shear. The softening behavior follow an exponential descending law defined by two parameters: the uniaxial tensile strength of concrete ($f_{ct}=3.5$ MPa) and fracture energy ($G_f=0.13$ N/mm), whose value is linked to the behavior more or less ductile element.

The nonlinear behavior in compression is governed by the following parameters: uniaxial compressive strength ($f_c=34.0$ MPa), strain at peak uniaxial compression ($\epsilon_c=0.00261$), biaxial to uniaxial stress ratio ($\beta_r=1.15$), initial relative position of yield surface ($Z_0=0.6$), dilatancy factor ($\psi=-0.1$), constant in interlock state function ($m_g=0.425$), contact multiplier on ϵ_0 for first opening stage ($m_{hi}=0.5$), final contact multiplier on ϵ_0 ($m_{hi}=15.0$), angular limit between crack planes ($\alpha_d=1.0$ rad). Further parameters are the shear intercept to tensile strength ($r_c=4.15$) and the slope of friction asymptote for damage ($\mu=1.3$) that define the surface of local damage. These values were assigned according to the suggestions provided by LUSAS manuals (LUSAS Finite

Element Analysis Ltd, version 14.5, 2010). Specifically, strain at peak uniaxial compression was estimated from $\epsilon_c=0.002+0.001((1.25f_c-15)/45)$.

3.4.2 Steel

The behavior of the steel in the linear elastic range is defined by the Young modulus ($E_s=210000$ MPa) and the Poisson ratio ($\nu_s=0.3$) while in the plastic range has been modeled according to the Von Mises criterion with strain hardening defined through the hardening yield strength (f_{sy}), the “slope” of strain hardening and ultimate plastic strain ($\epsilon_{su}=0.2$). Two different types of steel have been defined: tensile longitudinal reinforcement ($f_{sy}=604.2$ MPa, slope=1414.0 MPa) and compressed longitudinal reinforcement with the stirrups ($f_{sy}=496.0$ MPa, slope=1861.0 MPa), according to the mean values of the yield and maximum strength obtained through the laboratory tests.

3.4.3 SRG system

A linear elastic orthotropic behavior was assumed by defining the Young modules ($E_x=260000$ MPa, $E_y=E_z=12807$ MPa), the shear modules ($G_{xy}=G_{xz}=G_{yz}=7184$ MPa), and the Poisson ratios ($\nu_{xy}=\nu_{yz}=0.03$, $\nu_{xz}=0.215$) in the directions of the reference system.

3.4.4 Interface elements

The interface elements IS16 support a damage model called “Delamination Damage Model” characterized by three modes of failure, Opening, Sliding I and Sliding II (Fig. 5), the first due to normal stresses, while the other two depend on the shear stress. This model reproduces the non-linear behavior of a system containing the surfaces of potential delamination.

A linear behavior up to the initiation stress τ_{lim} , corresponding to the relative displacement s_{lim} , occurs. As this value is exceeded, a softening behavior, up to the fracture energy G_F release, occurs. The complete detachment occurs in correspondence of the opening distance s_{lo} . Each failure mode requires four input parameters: the initiation stress, the relative displacement, the fracture energy and the option which take into account the combined failure modes.

The value assigned to the above parameter is not easily determinable and, it is necessary to refer to the results of experimental tests such as those known as: single-lap, double-lap and shear tests, carried out on steel plates and FRP laminates. Furthermore, there are many interface law proposed in recent literature (Ombres 2012, Lu *et. al* 2005b, Monti *et. al* 2003, Savoia *et. al* 2003).

Some experimental and numerical analyses were carried out on cement based strengthening systems, in order to determine an analytical bond-slip model (D’Ambrisi *et al.* 2012, D’Ambrisi *et al.* 2013). However, extensive investigations have yet to be developed on this topic, also with reference to the SRG systems.

Generally, the values of τ_{lim} and G_F depend on the geometrical and mechanical properties of the concrete and external reinforcement system. The relationships used to calculate the input values for the FE analysis were proposed by Brosens and Van Gemert (1999). The tangential limit value τ_{lim} (N/mm²) can be evaluated by using the following relationship:

$$\tau_{lim} = k_b \cdot 1.80 \cdot f_{ct} \quad (1)$$

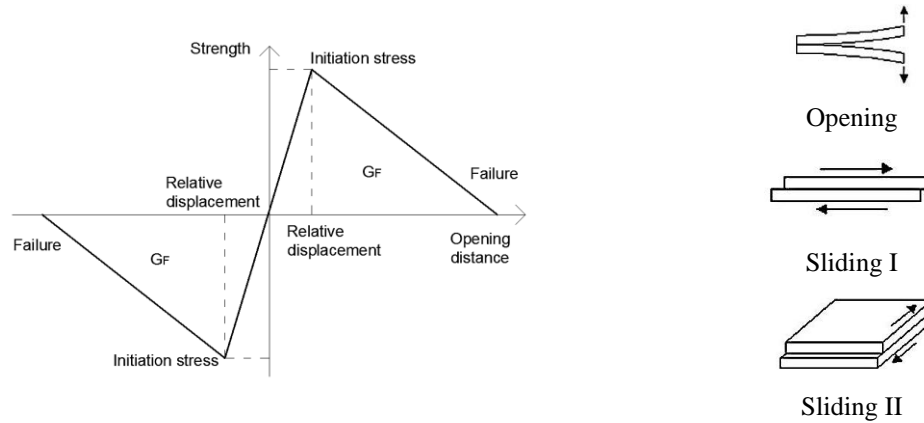


Fig. 5 “Delamination damage model” and fracture modes.

Table 2 “Delamination Damage Model” input parameters

Beam A1.A and A1.B	Fracture energy (N/mm)	0.63
	Initiation stress (N/mm ²)	4.88
	Relative displacement (mm)	0.000001
	Coupled/Uncoupled	Coupled

in which the parameter k_b takes into account the size of the reinforcement related to the size of the beam. The value of this parameter can be determined by the relationship:

$$k_b = \sqrt{\frac{k \cdot \left(2 - \frac{b}{B}\right)}{1 + \frac{b}{B_{10}}}} \quad (2)$$

in which b is the width of the external reinforcement (mm), B is the width of the concrete beam (mm), B_{10} is a reference value equal to 100 mm, and k is an empirical constant equal to 1.50. Here, a value of $k_b=0.775$ has been obtained.

The value of s_{lim} has little influence on the obtained numerical solution. A very small value of s_{lim} simulates a rigid interface. It can also be assumed equal to zero but in this study it was assumed $s_{lim}=0.000001$ mm.

The fracture energy, G_F , can be evaluated by using the following relationship:

$$G_F = k_b^2 \cdot C_f \cdot f_{ct} \quad (3)$$

The parameter C_f takes into account all the secondary effects and a value in the range 0.202-0.300 mm can be assigned. Here, a value of $C_f=0.300$ has been assumed.

In order to use in structural engineering field a simple yet rational model, this bond slip law was adapted.

In Table 2 are given the values of the input mechanical parameters of the “Delamination Damage Model” for the strengthened beams. These values calculated using the Eqs. (1)-(3) were assigned to the strengthened beams A1.A and A1.B, to the interface connections between SRG layer and concrete surface, at the bottom face and in the anchorage end regions.

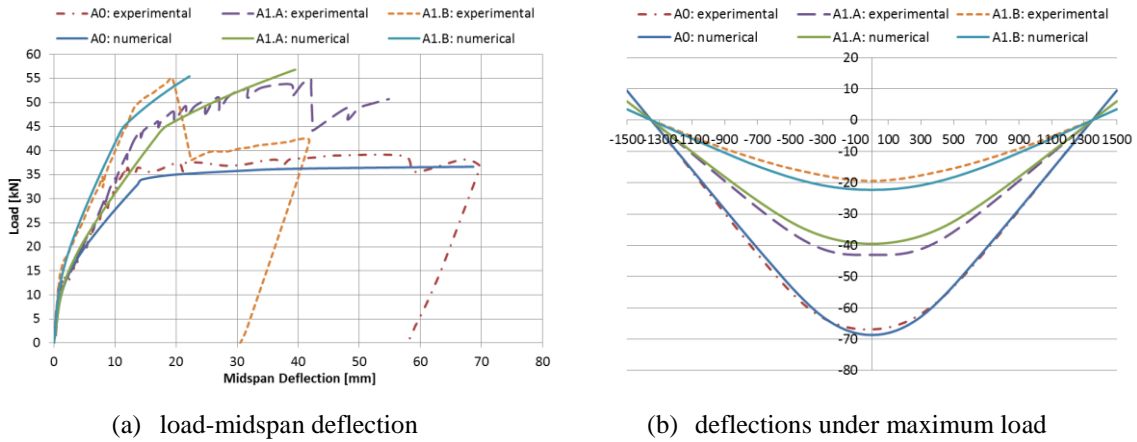


Fig. 6 Numerical/Experimental comparisons

Table 3 Numerical and experimental values of loads and ductility factors

Beam	Model	Load (kN)			Load factors		Deflection ductility factors	
		$F_{cracking}$	F_{yield}	$F_{ultimate}$	ΔF	Δ_F	μ_δ	Δ_δ
A0	Numerical	9.50	34.00	36.65	0.00	1.00	4.75	1.00
	Experimental	9.88	35.30	38.98	0.00	1.00	5.85	1.00
A1.A	Numerical	12.00	44.00	56.83	20.18	1.55	2.26	0.48
	Experimental	11.92	44.16	54.93	15.95	1.41	3.87	0.66
A1.B	Numerical	13.00	46.00	55.46	18.81	1.51	1.82	0.38
	Experimental	14.71	49.07	54.93	15.95	1.41	1.47	0.27

4. Experimental and numerical results

The Figs. 6(a)-(b) show the comparisons of the experimental and numerical results, in terms of load-midspan deflection curves and deflections under maximum load of the beams.

The Table 3 shows the load values at first crack ($F_{cracking}$), steel yield (F_{yield}), ultimate ($F_{ultimate}$). From the analysis of the above results the load and ductility factors of the three beams, numerical and experimental, were calculated. The values are also shown in Table 3, where ΔF is the difference between the ultimate load of each beam and that of the RC control beam A0; Δ_F is the ratio between the ultimate load of each beam with that of the RC control beam; μ_δ is the ratio between the deflection of the midspan section at failure and at yielding of the internal steel; Δ_δ is the ratio of the μ_δ of each beam with that of the RC control beam.

The results of the experimental investigation show that:

- The control beam A0 failed at an ultimate load of 38.98 kN, in a conventional ductile flexure mode with yielding of tension steel, followed by crushing of concrete in the compression zone. Its ductility index evaluated with reference to the midspan deflection was 5.85, very high.
- The strengthened beams A1.A and A1.B failed at an ultimate load equal to 54.93 kN for detachment of the external SRG system (“intermediate crack debonding” for beam A1.B and

“intermediate debonding followed by layer end debonding” for beam A1.A) with yielding of tension steel. The SRG system leads to an increase of the load carrying capacity of the RC beams ($\Delta F=15.95$ kN) and a decrease of deflection ductility index respect to the original un-reinforced RC beam.

- For the beam A1.B, to the load level of 45.00 kN a substantial cracking in the grout matrix was visible, the cracks in the bending region of the beam were almost vertical and extended up to about 200 mm of height from the bottom of the beam. To a load level of about 49.00 kN, the internal steel reached yield limit, a delamination began in the midspan zone and it grew until to the detachment of the reinforcing mesh, that occurred at the load level of about 55.00 kN. The beam had a sudden loss load capacity and afterwards its behavior was similar to that of the control beam A0.

- The beam A1.A with U-end anchorages and one layer of SRG reinforcing mesh had a greater deflections than the beam A1.B. The yielding of the internal steel occurred to a load level of 44.16 kN and the delamination phenomenon was delayed and thwarted by the U-end anchorages. Consequently, the beam reached the failure with the detachment of the reinforcing mesh and an unthreading from inside of the U-anchorage.

- The ductility index was equal to 3.87 and 1.47 for beams A1.A and A1.B, respectively (Table 3). The beam A1.A showed a more ductile behavior than that of the beam A1.B. The results showed in Figs. 6(a)-(b) confirm that the U-end anchorages enhance the deflection behavior. Indeed, the U-end anchorages enhance the ductility factor from a value of 0.27 to a value of 0.66 (Table 3).

These experimental results are reproduced in a satisfactory manner from the proposed FE 3D-model with a tolerance acceptable for the purpose of the present work (3.47% for the ultimate load values). Generally, the numerical values of the loads at the critical stages are slightly lower of the same loads experimentally detected. This shows that the 3D-model is reliable.

The results of the numerical analysis show that:

- for the control beam (beam A0) the analysis is stopped because of the achievement of the limit displacement of the control point;
- for the externally reinforced beams (A1.A and A1.B) the analysis stops before reaching the limit displacement of the control point because it reached strain limits in the materials. The reason of the stop is the same for both strengthened beams, and it is due to the full development of the interface model. In particular, for the beam A1.A, the shear stress limit ($\tau_{lm}=4.88$ N/mm²) is achieved in correspondence of the load equal to 29.0 kN, therefore all successive load increments will fall in the descending branch of the bi-linear curve of the “Delamination Damage Model” until to the achievement of the maximum displacement (s_{10}) recorded in correspondence of the ultimate load. For the beam A1.B, the shear stress limit ($\tau_{lm}=4.88$ N/mm²) is achieved in correspondence of load equal to 30.0 kN. Even in this case all successive load increments will fall in the descending branch of the bi-linear curve until reaching the maximum relative displacement (s_{10}) obtained in correspondence of the ultimate load. The maximum relative displacement is implicitly evaluated by fracture energy and shear stress limit ($s_{10}=2G_F/\tau_{lm}$).

5. Parametric study

The proposed FE 3D-model has been applied to investigate the effects of the concrete compressive strength and the amount of tensile steel reinforcement on the load carrying capacity

and the ductility of similar externally strengthened RC beams. Parameters that will influence the structural performance are certainly not limited to these. Nevertheless, the influences of other factors such as geometrical and mechanical properties of the external reinforcement SRG system are not addressed in this study, even though the 3D-model is able to analyze also these cases.

In particular, the values taken into consideration are:

- concrete compressive strength f_c : 20 MPa, 25 MPa, 32 MPa, 40 MPa;
- reinforcement ratio ρ : 0.00268 (2-8 mm dia), 0.00419 (2-10 mm dia).

The concrete compressive strengths have been chosen on the basis of concrete grades as provided by fib Model Code (2010). Specifically, low compressive strength (20 MPa and 25 MPa) and medium compressive strength (32 MPa and 40 MPa). The reinforcement ratios have been chosen lower (0.00268) and equal to the experimental value (0.00419). For each analysis, the value of the concrete tensile strength has been calculated as a function of the concrete compressive strength adopted, according to the relationship provided by fib Model Code (2010) $f_{ct}=0.3f_c^{2/3}$. Being f_{ct} known, the value of the input mechanical parameters of the “Delamination Damage Model” have been evaluated by Eqs. (1)-(3).

The results of the parametric study in terms of load-displacement curves, for the beams A0, A1.A and A1.B, to varying of the parameters listed above, are shown in Figs. 7-8.

In Table 4 are given the load values at steel yield (F_{yield}), ultimate ($F_{ultimate}$), and the load factors of all beams analyzed in the parametric study. In this case the ductility factors were not calculated, because it is not possible to perform a reliable comparison with the ductility of the control beams (the analysis was stopped specifying the maximum displacement’s value of a point on the middle section). An evaluation of the behavior more or less ductile of the strengthened beams is possible from the comparisons among the load-displacement curves obtained from the analyses.

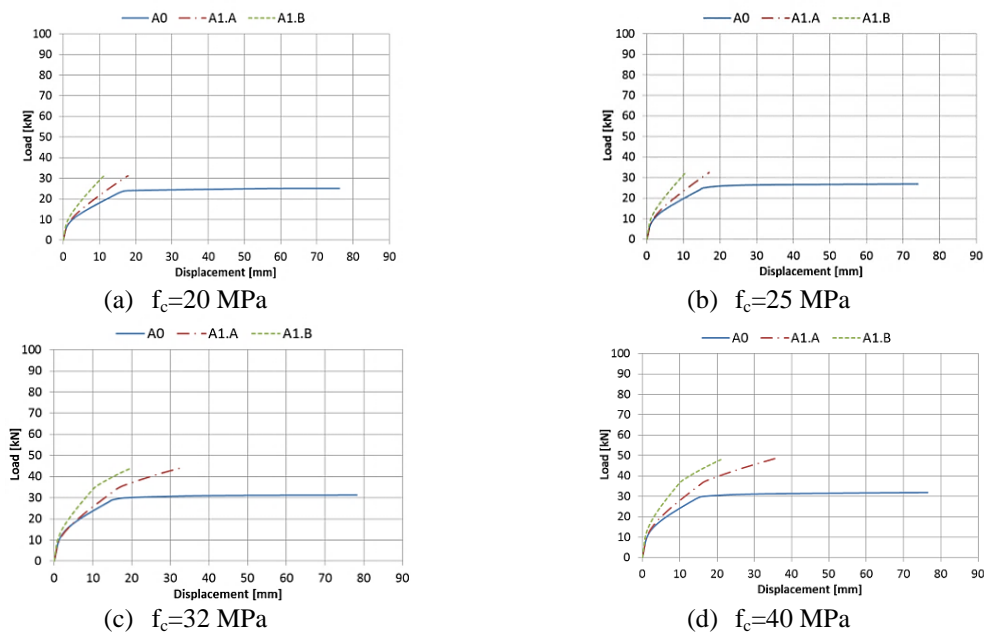


Fig. 7 Parametric study: $\rho=0.00268$

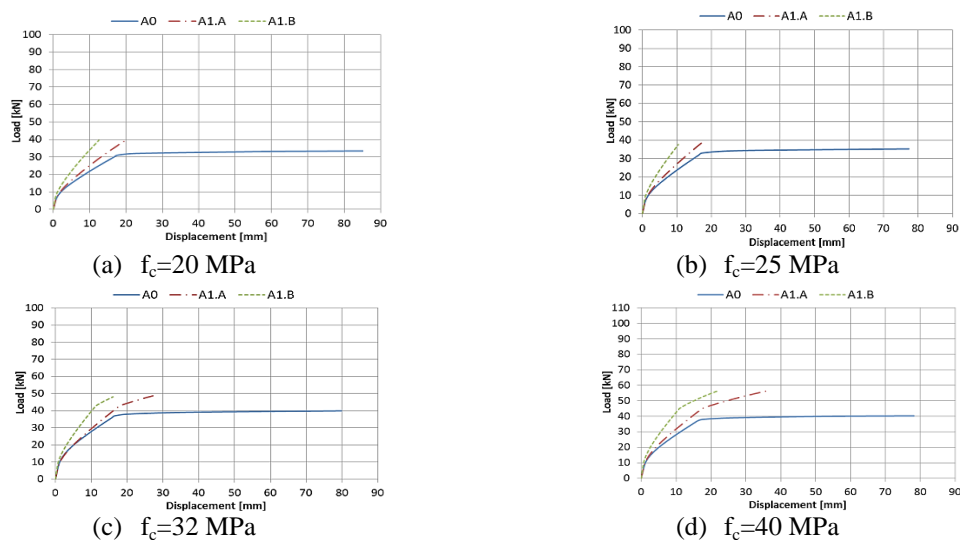
Fig. 8 Parametric study: $\rho=0.00419$

Table 4 Parametric study: numerical values of loads

BEAM	f_c	$\rho=0.00268$				$\rho=0.00419$			
		F_{yield}	$F_{ultimate}$	ΔF	Δ_F	F_{yield}	$F_{ultimate}$	ΔF	Δ_F
A0	20	23.00	25.12	0.00	1.00	31.00	33.45	0.00	1.00
A1.A		-	31.20	6.08	1.24	-	39.13	5.68	1.17
A1.B		-	31.18	6.06	1.24	-	39.07	5.62	1.17
A0	25	25.00	26.89	0.00	1.00	32.00	35.29	0.00	1.00
A1.A		-	32.50	5.61	1.21	-	38.67	3.38	1.10
A1.B		-	32.48	5.59	1.21	-	37.61	2.32	1.07
A0	32	29.00	31.25	0.00	1.00	37.00	39.90	0.00	1.00
A1.A		33.52	44.20	12.95	1.41	41.00	48.67	8.77	1.22
A1.B		34.50	44.17	12.92	1.41	41.25	48.07	8.17	1.20
A0	40	29.00	31.89	0.00	1.00	37.00	40.25	0.00	1.00
A1.A		36.11	48.52	16.63	1.52	42.25	56.60	16.35	1.41
A1.B		37.18	48.50	16.61	1.52	43.17	56.48	16.23	1.40

In general, the results of the parametric study show that the application of the external reinforcement, with and without U-end anchorages, not always improves the structural performance. Indeed, in all cases, the SRG system leads to an increase of the load carrying capacity of the RC beams (Δ_F varies in the range of 1.10 – 1.50), and a decrease of deflections respect to the original un-reinforced RC beam.

The structural behavior of the externally reinforced RC beams is similar (Figs. 7-8). In fact, the strengthened beams, with and without U-end anchorages, have achieved the failure for detachment of the external reinforcement, in some case before yielding of the tensile steel (low grade concrete, $f_c=20$ MPa and 25 MPa) in other case after yielding of the tensile steel (medium grade concrete, $f_c=32$ MPa and 40 MPa).

6. Conclusions

The work developed shows that the numerical model built is able to identify the structural behavior of the RC beams strengthened with SRG system up to failure. In fact, the comparison between the experimental and numerical results has proved to be satisfactory.

This allows to evaluate numerically the behavior of the RC strengthened beams under increasing load until failure without carrying out experimental testing. In fact, the parametric analysis carried out showed the efficiency of the model to predict the behavior of strengthened beams, with and without U-end anchorages, when the concrete compressive strength and the amount of internal steel reinforcement ratio varied. The study shows that:

- the beams strengthened with a layer of SRG system, with and without U-end anchorages, have a brittle structural behavior, respect to the control beams, in some cases with tensile steel yielding ($f_c=32$ MPa and 40 MPa), in other cases without tensile steel yielding ($f_c=20$ MPa and 25 MPa);
- the load carrying capacity of the RC strengthened beams is quite similar for both the beams with and without U-end anchorages;
- the additional U-end anchorages reduce the slip between the external system and the concrete tensile face of the beam, and allow in all cases a better structural performance in terms of deflections and deformability of the strengthened beams;
- a concrete of better quality and good strength assures the yielding of the internal steel, even with different amount, before that the detachment of the SRG strengthening system with loss of load capacity occurs.

The SRG system is a reliable technology for the external reinforcement of existing RC beams if an increase of load carrying capacity of the structural elements is required. To have a ductile behavior at ultimate stage, under increasing load, the reinforcing mesh of the SRG system should be effectively anchored to the concrete beam substrate, but for concretes with low strength grade this is not enough.

References

- ACI 440.2R-08 (2008), *Guide for the Design and Construction of Externally Bonded FRP Systems for Strengthening Concrete Structures*, American Concrete Institute, Farmington Hills, Michigan, USA.
- Barton, B., Wobbe, E., Dharani, L.R., Silva, P., Birman, V., Nanni, A., Alkhrdaji, T., Thomas, J. and Tunis, G. (2005), "Characterization of reinforced concrete beams strengthened by steel reinforced polymer and grout (SRP and SRG) composites", *Mater. Sci. Eng. A*, **412**(1-2), 129-136.
- Bazant, Z.P. and Oh, B. (1983), "Crack band theory for fracture of concrete", *Mater. Struct.*, **16**(3), 155-177.
- Bencardino, F., Spadea, G. and Swamy, R.N. (2002), "Strength and ductility of reinforced concrete beams externally reinforced with carbon fiber fabric", *ACI Struct. J.*, **99**(2), 163-171.
- Bencardino, F., Colotti, V., Spadea, G. and Swamy, R.N. (2005), "Shear behavior of reinforced concrete beams strengthened in flexure with bonded carbon fibre reinforced polymers laminates", *Can. J. Civil Eng.*, **32**(5), 812-824.
- Bencardino, F., Spadea, G. and Swamy, R.N. (2007), "The problem of shear in RC beams strengthened with CFRP laminates", *Construct. Build. Mater.*, **21**(11), 1997-2006.
- Bencardino, F. and Spadea, G. (2014), "FE modeling of RC beams externally strengthened with innovative

- materials”, *Mechanics Research Communications*, **58**, 88-96.
- Brosens, K. and Van Gemert, D. (1999), “Anchorage design for externally bonded carbon fiber reinforced polymer laminates”, *Proceedings of the 4th International Symposium on FRP Reinforcement for Concrete Structures*, ACI International SP 188-56, 635-645, Baltimore, MD, November.
- Casadei, P., Nanni, A. and Alkhrdaji, T. (2005a), “Steel-reinforced polymer: an innovative and promising material for strengthening infrastructures”, *Concrete Eng. Int.*, **9**(1), 54-56.
- Casadei, P., Nanni, A., Alkhrdaji, T. and Thomas, J. (2005b), “Performance of double-T prestressed concrete beams strengthened with steel reinforced polymer”, *Adv. Struct. Eng.*, **8**(4), 427-441.
- CNR-DT 200 R1/2013 (2013), *Guide for the Design and Construction of Externally Bonded FRP Systems for Strengthening Existing Structures – Materials, RC and PC structures, masonry structures*, Italian National Research Council, Rome, Italy.
- D’Ambrisi, A., Feo, L. and Focacci, F. (2012), “Bond-slip relations for PBO-FRCM materials externally bonded to concrete”, *Compos. Part B: Eng.*, **43**, 2938–2949.
- D’Ambrisi, A., Feo, L. and Focacci, F. (2013), “Experimental analysis on bond between PBO-FRCM strengthening materials and concrete”, *Compos. Part B: Eng.*, **44**, 524-532.
- Demakos, C.B., Repapis, C.C. and Drivas, D. (2013), “Investigation of structural response of reinforced concrete beams strengthened with anchored FRPs”, *The Open Construction and Building Technology Journal*, **7**, 146-157.
- Ferracuti, B., Savoia, M. and Mazzotti, C. (2006), “A numerical model for FRP-concrete delamination”, *Compos. Part B: Eng.*, **37**, 256-364.
- Ebead, U. and Saeed, H. (2014), “Numerical modeling of shear strengthened reinforced concrete beams using different systems”, *J. Compos. Construct.*, **18**(1), 04013031(11).
- Eurocode 2 (2004), “*Design of Concrete Structures – Part 1-1: General Rules and Rules for Buildings*”, EN 1992-1-1: 2004, European Committee for Standardization.
- Fib Model Code (2010), *Fib model code for concrete structures 2010*, Fib Bulletin No. 65 and 66, fib (CEB-FIP), Lausanne, Switzerland.
- Fib 14 (2001), *Externally bonded FRP reinforcement for RC structures*, Technical Report Bulletin No. 14, fib (CEB-FIP), Lausanne, Switzerland.
- Fib 35 (2006), *Retrofitting of concrete structures by externally bonded FRPs with emphasis on seismic applications*, Technical Report Bulletin No. 35, fib (CEB-FIP), Lausanne, Switzerland.
- Huang, X., Birman, V., Nanni, A., and Tunis, G. (2004), “Properties and potential for application of steel reinforced polymer and steel reinforced grout composites”, *Compos. Part B: Eng.*, **36**(1), 73-82.
- ISIS Design manual No. 4, *FRP rehabilitation of reinforced concrete structures*, ISIS Canada.
- Jumaat, M.Z. and Ashraf Al Alam, M.D. (2010), “Experimental and numerical analysis of end anchored steel plate and CFRP laminate flexurally strengthened reinforced concrete (r. c.) beams”, *Int. J. Phys. Sci.*, **5**(2), 132-144.
- Kimia S.A. (2009), *Unidirectional high-strength carbon steel fibre reinforcing mesh*, Kimisteel 1500, ST2-0610, *Ready-to-use fine granulometry mortar for SRG systems*, Kimisteel LM, ST2-0610, *Synthetic resin used specifically to improve the chemical and physical properties of single-component mortars*, Kimitech B2, ST9-0607.
- Lopez, A., Galati, N., Alkhrdaji, T. and Nanni, A. (2007), “Strengthening of a reinforced concrete bridge with externally bonded steel reinforced polymer (SRP)”, *Composites Part B: Eng.*, **38**(4), 429-436.
- Lu, X.Z., Ye, L.P., Teng, J.G. and Jiang, J.J. (2005a). “Meso-scale finite element model for FRP sheets/plates bonded to concrete”, *Eng. Struct.*, **27**(4), 564–575.
- Lu, X.Z., Teng, J.G., Yea, L.P. and Jiang, J.J. (2005b), “Bond-slip models for FRP sheets/plates bonded to concrete”, *Eng. Struct.*, **27**, 920–937.
- LUSAS Finite Element Analysis Ltd, version 14.5 (2010), “engineering analysis software”, “theory manual 1”, “theory manual 2”, “element reference manual”, Forge House, 66 High Street, Kingston upon Thames, Surrey, KT1 1HN, United Kingdom.
- Monti, M., Renzelli, M. and Luciani, P. (2003), “FRP adhesion in uncracked and cracked concrete zones”, *Proceedings of the 6th International Symposium on FRP Reinforcement for Concrete Structures*,

Singapore, July.

- Ombres, L. (2012), "Debonding analysis of reinforced concrete beams strengthened with fibre reinforced cementitious mortar", *Eng. Fract. Mech.*, **81**, 94–109.
- Pecce, M., Ceroni, F., Prota, A. and Manfredi, G. (2006), "Response prediction of RC beams externally bonded with steel-reinforced polymers", *J. Compos. Construct.*, **10**(3), 195-203.
- Prota, A., Tan, K.Y., Nanni, A., Manfredi, G. and Pecce, M. (2006), "Performance of RC shallow beams externally bonded with steel reinforced polymer", *ACI Struct. J.*, **103**(2), 163-170.
- Savoia, M., Farracuti, B. and Mazzotti, D. (2003), "Non-linear bond-slip law for FRP-concrete interface", *Proceedings of the 6th international symposium on FRP reinforcement for concrete structures*, 163–72.
- Spadea, G., Bencardino, F. and Swamy, R.N. (2000), "Optimizing the performance characteristics of beams strengthened with bonded CFRP laminates", *Mater. Struct.*, **33**(226), 119-126.
- Wobbe, E., Silva, P.F., Barton, B.L., Dharani, L.R., Birman, V., Nanni, A., Alkhrdaji, T., Thomas, J. and Tunis, T. (2004), "Flexural capacity of RC beams externally bonded with SRP and SRG", *Proceedings of the Society for the Advancement of Materials and Process Engineering, International, Symposium and Exhibition*, Long Beach, Ca, May.
- Zhang, L. and Teng, J.G. (2010), "Finite element prediction of interfacial stresses in structural members bonded with a thin plate", *Eng. Struct.*, **32**, 459-471.

CC